Spatial Investigation of Transverse Mode Turn-On Dynamics in VCSELs

Safwat W.Z. Mahmoud

Data transmission experiments with single-mode as well as multimode 850 nm VCSELs are carried out from a near-field point of view. Special attention is paid to important quantities like on/off-ratio and bit error rate (BER). A single-mode VCSEL oscillating on the fundamental LP_{01} mode shows no change in eye opening, on/off-ratio, and BER at different lateral fiber coupling positions. In case of a multimode VCSEL oscillating both on the LP_{01} mode and LP_{11} donut mode we observe a significant lateral change in the on/off-ratio which plays an important role in BER measurements.

1. Introduction

A light source of great scientific and commercial interest is the vertical-cavity surface-emitting laser (VCSEL) because it offers a number of favorable properties like low lasing threshold current [1], dynamic single-mode operation [2], low divergence circular beams [3], high packing density [4], and high-speed current modulation for multi-Gb/s data generation [5]. Despite these attractive features, the complex transverse modal behavior of VCSELs at high pump rates and large active diameters is a major drawback mainly in datacom applications. The mode dynamics are strongly dependent on the spatial carrier distribution which itself is governed by the influence of pump induced current spreading, hole burning, and thermal gradients in the laser cavity [6], [7]. The details of the transverse mode pattern in the device are of concern especially for fiber coupling where today both single-mode and multimode VCSEL approaches are followed in combination with a graded-index multimode fiber (MMF). In addition, the laser turn-on event depends on the driving current and consequently can be expected to be influenced by the device's transverse mode structure. In this work we employ near-field measurements to investigate the spectral and spatial intensity distribution of transverse modes in VCSELs with 4 and 6 μm active diameters. We use the same approach to perform bit error measurements at moderate bit rates of 1 and 2.5 Gb/s for different lateral fiber coupling offsets.

2. Device Structure and Output Characteristics

The layer structure of the selectively oxidized top-emitting VCSELs used in this work is grown by solid source molecular beam epitaxy. The active region is formed by three 8 nm

thick GaAs quantum wells embedded in $Al_{0.2}Ga_{0.8}As$ barriers for about 850 nm gain peak wavelength. The carbon doped p-type and silicon doped n-type Bragg reflectors consist of 19 and 35.5 $Al_{0.1}Ga_{0.9}As/Al_{0.9}Ga_{0.1}As$ pairs, respectively. For lateral current confinement, a single 25 nm thick AlAs layer is placed in the first quarter wavelength layer above the active zone and is subsequently oxidized after a mesa etching process. In Fig. 1 the light output characteristics of 4 μm (solid curves) and 6 μm (dashed curves) aperture diameter selectively oxidized VCSELs are depicted. The smaller device has a threshold current of 0.7 mA and emits in a single mode, as shown in Fig. 2(b). The threshold current of the larger device is 1.1 mA and it starts lasing on the fundamental mode up to 1.5 mA, then becomes multimode for higher currents as illustrated in Fig. 2(d).

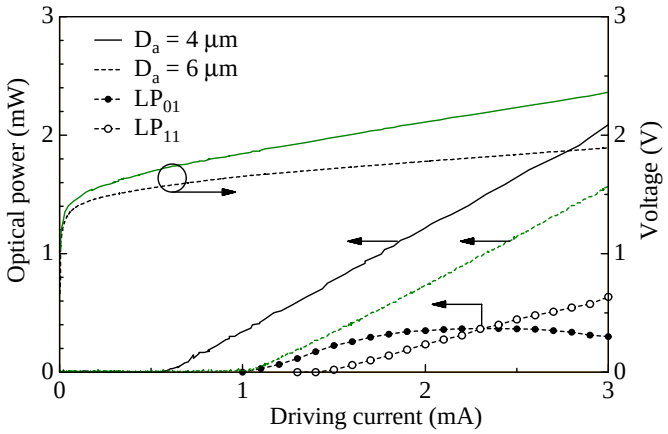

Fig. 1. Light-current and current-voltage characteristics of 4 μm (solid curves) and 6 μm (dashed curves) aperture oxide-confined VCSELs. The closed and open circles define the peak spectral power emitted from the larger device in the LP_{01} and LP_{11} modes, respectively.

To analyze the spatial profiles of the lasing modes we have carried out near-field measurements based on a single-mode fiber (SMF) tip scanning technique [8]. Fig. 2(a) shows a transverse central cross-section of the measured near-field intensity profile of the Gaussian-like transverse fundamental LP_{01} mode (solid circles) for the VCSEL with active diameter $D_a = 4\,\mu$m at 2 mA bias current and 300 mV modulation voltage of a 1 Gb/s data rate pseudo-random bit sequence (PRBS) signal. Under these conditions, emission is single-mode with a sidemode suppression ratio of better than 30 dB, as illustrated in Fig. 2(b). The same measurements for the VCSEL with $D_a = 6\,\mu$m at 2 mA bias current and 150 mV modulation voltage are illustrated in Fig. 2(c). In this case the increase of the active diameter leads to the excitation of both LP_{01} mode (solid circles) and the higher order transverse LP_{11} mode (open circles). Both modes are circularly symmetric with the LP_{11} mode exhibiting an intensity dip in the center of the cavity. The emission spectrum in Fig. 2(d) shows that the LP_{11} mode is blue shifted from the LP_{01} mode by 0.4 nm.

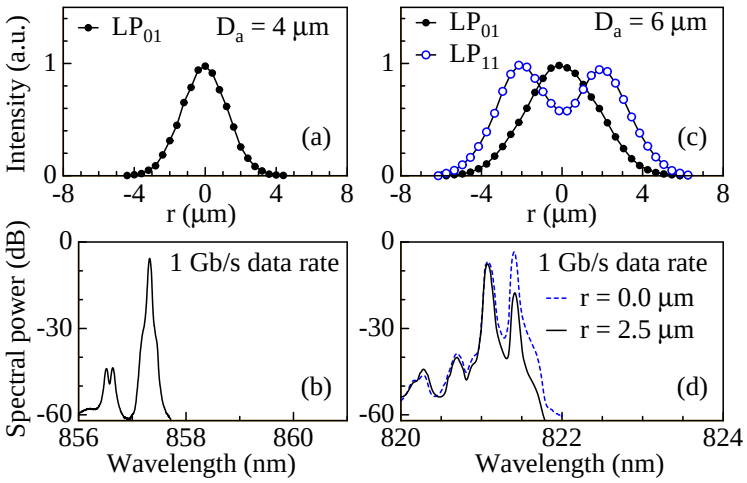

Fig. 2. Spatial intensity distribution and emitted spectrum of a 4 μm aperture device at 2 mA bias current and 300 mV modulation voltage (a) and (b). The results of the same measurements on a 6 μm aperture device at 2 mA bias current and 150 mV modulation voltage are displayed in (c) and (d), where the additional spectrum in (d) is taken for 2.5 μm radial fiber offset.

3. Data Transmission

To investigate data transmission at different lateral positions of the fiber relative to the VCSEL center, we employed a SMF tip near-field scanning system in combination with a data transmission setup [5], using a 2 GHz bandwidth germanium avalanche photodiode as a receiver. The bias current of 2 mA and a 1 Gb/s PRBS signal of 2^7-1 word length and modulation voltage $V_{pp} = 300$ mV were combined in a bias-tee and fed to the VCSEL of $D_a = 4\,\mu$m. The results of the data transmission experiments using the 2 m length SMF whose tip has a semispherical lens or using a 5 m length, 50 μm core diameter MMF are summarized in Fig. 3. The eye diagrams in the inset show that as the SMF tip is moved laterally from the center at a radial position r = 0 to the edge of the LP_{01} mode at r = 2 μm, the eye remains symmetric and has the same form as with the MMF. The received power for a BER of 10^{-11} is about -19 dBm for both SMF and MMF. The radial distribution of the on/off-ratio (P_{on}/P_{off}) is obtained from a sampling oscilloscope by dividing the average values of histograms on both the "1" and "0" rails of the eye diagram. The closed squares in Fig. 4 reveal a nearly constant ratio of 9 dB which is the same value as obtained by using the MMF.

In case of the multimode VCSEL, the same bias current and modulation signal, however with $V_{pp} = 150$ mV, are chosen. In accordance with the emission spectrum in Fig. 2(d), at the center both LP_{01} and LP_{11} modal power is coupled into the SMF. As the tip is moved toward the edge of the VCSEL, the LP_{01} mode is strongly attenuated and shows 10 dB suppression ratio in the interval between r = 2.5 . . . 3.5 μm. This is evidenced in the results of the data transmission experiments in Fig. 5 using the forementioned fibers. The eye diagrams in the inset show that at r = 0 the eye is no longer symmetric because

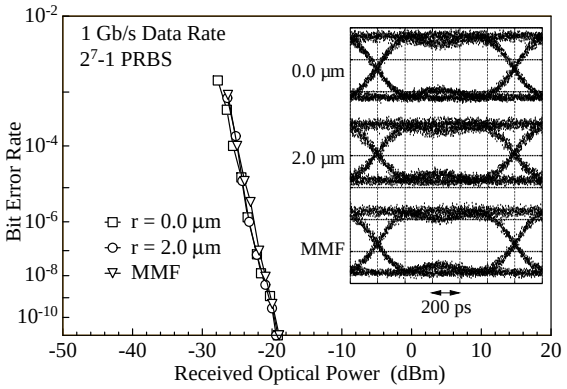

Fig. 3. Bit error measurements using a 2 m length SMF at two different radial positions or using 5 m MMF. The 4 μm aperture VCSEL is fed with 2 mA dc and 1 Gb/s PRBS signals at a word length of $2^7 - 1$ and $V_{pp} = 300$ mV. The corresponding eye diagrams are recorded at 10^{-11} BER.

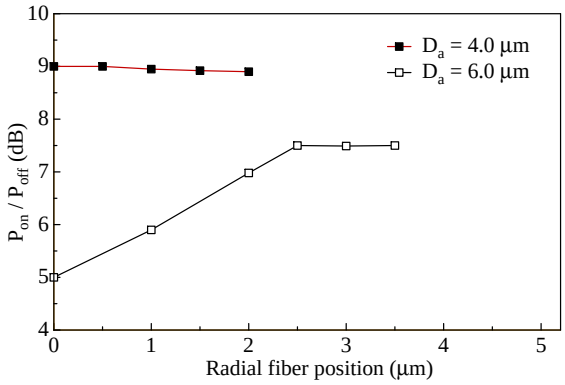

Fig. 4. Spatial on/off-ratio distribution for a 4 μm aperture VCSEL (closed squares) under the same conditions as in Fig. 3 and for a 6 μm aperture device (open squares) under the same conditions as in Fig. 5.

the LP_{01} and LP_{11} modes are both coupled into the SMF. Since the LP_{11} mode has a higher threshold current, as seen in Fig. 1, it has a lower resonance frequency at the same bias current and as a result gives rise to ringing in the eye diagram. At r = 2.5 μm, the dominance of LP_{11} at a sidemode suppression in the order of 10 dB gives a symmetric eye opening with a longer switch-on time than at r = 0, as expected. These conclusions are supported by the results of theoretical simulations performed in [9]. In calculations of the time traces of the LP_{11} and LP_{01} modal powers it was found that the latter has a shorter turn-on delay and accordingly the LP_{01} mode starts lasing emission. When a significant number of photons are present in the laser microcavity, a hole is burnt in the carrier profile which leads to the excitation of the higher order LP_{11} mode. Using a MMF, a superposition of all portions of the two modes gives an eye diagram with symmetric opening. The BER curves show that the received optical power for a BER of 10^{-11} is -16.6 dBm for the SMF at r = 2.5 μm with a power penalty of 3.3 dB at r = 0 and of 2.1 dB for the MMF. This difference is attributed to the radial change of P_{on}/P_{off}, as illustrated in Fig. 4 (open squares). The on/off-ratio is continually increasing up to r = 2.5 μm where it reaches a constant value of about 7.5 dB, while 6.5 dB ratio is recorded for the MMF. These results are also confirmed by the separate light-current characteristics in Fig. 1 which are obtained from the spectrometer as the peak spectral power of each mode. In accordance with these curves, the average differential efficiency for the LP_{01} mode is smaller than for LP_{11} in the interval around 2 mA at which the VCSEL is modulated. The data transmission experiments are repeated with the same multimode VCSEL and fibers for 2.5 Gb/s data rate and are summarized in Fig. 6. The same effects as in the case of 1 Gb/s data transmission are seen, but a BER floor at 10^{-8} is observed at r = 0 because the "1" rail in the eye diagram exhibits much noise which

reduces its opening. This increased noise is probably due to mode partition because as the total optical power remains constant, the relative distribution of the modal powers fluctuates as shown in Fig. 1.

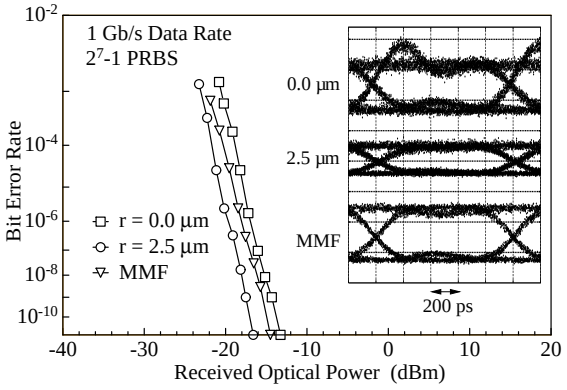

Fig. 5. Bit error measurements using 2 m SMF at different radial positions defined by the legends or 5 m MMF for a 6 μm aperture device fed with 2 mA dc and 1 Gb/s PRBS signal at a word length 2^7-1 and $V_{pp} = 150$ mV. The corresponding eye diagrams are recorded at 10^{-11} BER.

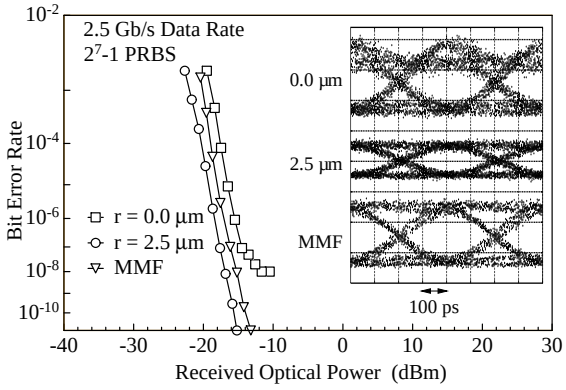

Fig. 6. The same measurements as in Fig. 5 at 2.5 Gb/s data rate. The eye diagrams are recorded at the minimum BER for each case.

4. Conclusion

We have measured spectral as well as spatial intensity distributions of the eigenmodes for single-mode and multimode VCSELs under modulation. Bit error rate measurements at 1 Gb/s and 2.5 Gb/s for these devices have been presented for different lateral SMF offsets which point to a better performance of single-mode compared with multimode VCSELs. The multimode device has shown a lateral variation of the on/off-ratio which leads to a reduced BER for the LP_{11} mode at 10 dB LP_{01} suppression than when the two modes coexist. We conclude from these results that at moderate bit rates the on/off-ratio is the dominant mechanism governing the BER measurements regardless of the type of oscillating mode in the cavity. The difference between the switch-on times of the lasing modes in the multimode device can be of importance even at high bit rates.

References

[1] D.G. Deppe, D.L. Huffaker, T. Oh, H. Deng, and Q. Deng "*Low-threshold vertical-cavity surface-emitting lasers based on oxide-confined and high contrast distributed Bragg reflectors,*" IEEE J. Selected Topics Quantum Electron., vol. 3, pp. 893–904, 1997.

[2] C. Jung, R. Jäger, P. Schnitzer, R. Michalzik, B. Weigl, S. Müller, and K.J. Ebeling "*4.8 mW single-mode oxide confined top-surface emitting vertical-cavity laser diodes,*" Electron. Lett., vol. 32, pp. 1790–1791, 1997.

[3] D.G. Deppe and D.L. Huffaker, "*High spatial coherence vertical-cavity surface-emitting laser using a long monolithic cavity,*" Electron. Lett., vol. 33, pp. 211–213, 1997.

[4] R. King, R. Michalzik, C. Jung, M. Grabherr, F. Eberhard, R. Jäger, P. Schnitzer, and K.J. Ebeling "*Oxide confined 2D VCSEL arrays for high-density inter/intra-chip interconnects,*" Proc. SPIE, vol. 3286, pp. 64–67, 1998.

[5] D. Wiedenmann, R. King, C. Jung, R. Jäger, P. Schnitzer, R. Michalzik, and K.J. Ebeling "*Design and analysis of single-mode oxidized VCSEL's for high-speed optical interconnects,*" IEEE J. Quantum Electron., vol. 5, pp. 503–511, 1999.

[6] C. Deng, I. Fischer, and W. Elsäßer, "*Transverse modes in oxide confined VCSELs: Influence of pump profile, spatial hole burning, and thermal effects,*" Optics Express, vol. 5, pp. 38–47, 1999.

[7] Y.G. Zhao and J. McInerney, "*Transverse-mode control of vertical-cavity surface-emitting lasers,*" IEEE. J. Quantum Electron., vol. 32, pp. 1950–1958, 1996.

[8] S.W.Z. Mahmoud, H. Unold, W. Schmid, R. Jäger, R. Michalzik, and K.J. Ebeling, "*Analysis of longitudinal mode wave guiding in vertical-cavity surface-emitting lasers with long monolithic cavity*", Appl. Phys. Lett., vol. 78, pp. 586–588, 2001.

[9] J. Dellunde, M.C. Torrent, J.M. Sancho, and K.A. Shore, "*Statistics of transverse-mode turn-on dynamics in VCSEL's*", IEEE J. Quantum Electron., vol. 33, pp. 1197–1204, 1997.